Quaternary Science Reviews 75 (2013) 1–10

Contents lists available at SciVerse ScienceDirect

Quaternary Science Reviews

journal homepage: www.elsevier.com/locate/quascirev

High-resolution variability of the South American summer monsoon over the last seven millennia: insights from a speleothem record from the central Peruvian Andes

Lisa C. Kanner [a,*], Stephen J. Burns [a], Hai Cheng [b,c], R. Lawrence Edwards [c], Mathias Vuille [d]

[a] Department of Geosciences, University of Massachusetts, Amherst, MA 01002, USA
[b] Institute of Global Environmental Change, Xi'an Jiaotong University, Xi'an 710049, China
[c] Department of Geology and Geophysics, University of Minnesota, Minneapolis, MN 55455, USA
[d] Department of Atmospheric and Environmental Sciences, University at Albany, State University of New York, Albany, NY 12222, USA

ARTICLE INFO

Article history:
Received 11 September 2012
Received in revised form
10 May 2013
Accepted 12 May 2013
Available online

Keywords:
Speleothem
South American summer monsoon
El Niño–Southern Oscillation
Peruvian Andes
Oxygen isotopes

ABSTRACT

Stable oxygen isotope ($\delta^{18}O$) measurements of two speleothems, collected from Huagapo Cave in the central Peruvian Andes and with overlapping age from 1.1 to 1.4 ka, characterize tropical South American climate variability over the last 7150 years. In the study region, precipitation $\delta^{18}O$ ($\delta^{18}O_p$) is inversely correlated to rainfall amount upstream in the Amazon Basin and the intensity of convection associated with the South American summer monsoon (SASM). Speleothem long-axis profiles yield an average age resolution of five years and permit investigation of climate over orbital to decadal timescales. Variations in the isotopic composition of Huagapo Cave calcite ($\delta^{18}O_c$) are in good agreement with several precipitation proxy records from ice cores, speleothems, and lake sediments from the central Peruvian Andes. From the mid-Holocene to today, $\delta^{18}O_c$, a proxy for $\delta^{18}O_p$, tracks changes in local insolation and exhibits a ~2‰ decrease. In the Late Holocene, Huagapo Cave $\delta^{18}O_c$ is characterized by two periods of significant decline in SASM intensity (up to 1.5‰ increase in $\delta^{18}O_c$) even when insolation is reaching a local maximum and the SASM would be expected to intensify. These millennial-scale reductions in SASM intensity could in part be influenced by a reduction in the zonal SST gradient of the Pacific Ocean, favoring El Niño-like development.

1. Introduction

Climate variability in the Peruvian Andes over the Holocene has been characterized through a variety of paleoclimate proxies including glacial ice cores (Thompson et al., 1984, 2000), glacial moraines (Smith and Rodbell, 2010), lake sediments (Abbott et al., 1997; Seltzer et al., 2000; Abbott et al., 2003; Bird et al., 2011a), and speleothems (vanBreukelen et al., 2008; Reuter et al., 2009). These archives have been variably interpreted in terms of temperature (Thompson et al., 1986, 2006; vanBreukelen et al., 2008), changes in precipitation amount locally (Seltzer et al., 2000) and upstream along the moisture transport pathway (Hoffmann et al., 2003). Independent of whether these records primarily reflect temperature or precipitation, they demonstrate that tropical South American climate is sensitive to atmospheric and oceanic parameters over short and long timescales. Orbital-scale trends are forced by austral summer insolation (Thompson et al., 1995; Seltzer et al., 2000), while centennial to decadal scale variance has been linked to Northern Hemisphere temperatures (Bird et al., 2011b), the El Niño–Southern Oscillation (ENSO) and state of the tropical Pacific (Thompson et al., 1984; Bradley et al., 2003), and sea surface temperatures (SSTs) in the tropical Atlantic Ocean (Reuter et al., 2009).

The breadth of precipitation $\delta^{18}O$ proxies from the region has recently allowed for the discussion of a coherent history of tropical South American climate over the last two millennia (Vuille et al., 2012). High-resolution stable isotope proxies from speleothems, ice cores, and lake sediments located within the South American monsoon belt demonstrate similar variations in monsoon strength over centennial and multidecadal timescales. During the last two thousand years, mean state changes in the monsoon variability were noted during three key intervals, the Medieval Climate Anomaly (MCA), the Little Ice Age (LIA), and the Common Warm Period (CWP). During the LIA, the proxy records contain the lightest $\delta^{18}O$ values, indicative that South American summer monsoon

* Corresponding author. Current address: University of Southern California, Department of Earth Sciences, 3651 Trousdale Parkway, Los Angeles, CA 90089, USA. Tel.: +1 213 740 6733.
E-mail address: lkanner@usc.edu (L.C. Kanner).

0277-3791/$ – see front matter © 2013 Elsevier Ltd. All rights reserved.
http://dx.doi.org/10.1016/j.quascirev.2013.05.008

(SASM) convection and rainout strengthened at that time. For the periods of the MCA and CWP on the other hand, $\delta^{18}O$ values are shifted to heavier values, suggesting a weaker monsoon. Vuille et al. (2012) proposed that these mean-state changes were related in part to North Atlantic climate variability, including Northern Hemisphere temperature anomalies, the strength of the Atlantic Multidecadal Oscillation (AMO), and the latitudinal position of the Atlantic Intertropical Convergence Zone (ITCZ).

While there is good correspondence between proxy records in the Late Holocene, the characterization of regional-scale and sub-orbital climate fluctuations beyond the last two thousand years, however, has not been established. In particular, the forces on SASM variability on sub-orbital timescales throughout the Holocene are not certain. North Atlantic climate variations can in part explain Late Holocene centennial-scale fluctuations (Vuille et al., 2012), but that influence may not extend to earlier in the Holocene when there were changes in the insolation-driven seasonal cycle. Another potential influence on tropical Andean climate and the SASM for sub-orbital timescales is ENSO. Even though centennial-scale changes in ENSO are subordinate to North Atlantic fluctuations in the Late Holocene (Vuille et al., 2012), ENSO driven changes are captured in the modern interannual isotopic signatures of SASM variations (Vuille and Werner, 2005) and Andean ice cap accumulation rates (Bradley et al., 2003). Thus, where high-resolution proxy records permit, it could be possible to detect interannual El Niño/La Niña cycles outside of the modern era. Furthermore, mean-state, millennial-scale variations in ENSO-like behavior have also been proposed for the last several thousand years. Sediment flux records from lakes in the Galapagos and Ecuador indicate a large growth in ENSO variance 2–3 thousand years ago (Moy et al., 2002; Conroy et al., 2008) and orbitally forced climate model simulations support increased ENSO variability in the Late Holocene compared to the mid and early Holocene (Clement et al., 2000; Luan et al., 2012). Whether the mean-state changes in ENSO detected in tropical Pacific records extend to the Andes and the SASM remains uncertain.

Here, we present results from a precisely dated stalagmite record from the central Peruvian Andes (11.27°S; 75.79°W, ~3850 m above sea level) to investigate interannual to millennial-scale climate variance over the Holocene. The oxygen isotopic composition of speleothem calcite is measured along the growth axis and is developed as a proxy for precipitation $\delta^{18}O$. Using this precisely dated and high-resolution reconstruction we characterize regional-scale changes in climate of the Peruvian Andes and attempt to untangle the influences of zonal (ENSO) and meridional (ITCZ) forcings of the tropical climate system at different timescales. Finally, this longer reconstruction offers perspective on the coherent centennial-scale changes recently observed from the range of SASM isotopic proxies of the last two millennia.

2. Modern climatology of tropical South America

Tropical South American climate is dominated by large seasonal changes in precipitation primarily related to the development of the SASM, which reaches its maximum intensity in terms of convection and rainout during the austral summer. During this mature phase of the SASM, the ITCZ has shifted to its most southerly position and the land-sea temperature contrast is at its height. The south-central portion of the Amazon Basin also receives its greatest rainfall as a result of a continental low-pressure system, the Chaco Low, which forms over northwestern Argentina (Seluchi et al., 2003). In connection with an upper-level, high-pressure system, the Bolivian High that forms to the southwest of the Amazon Basin (Lenters and Cook, 1997), mid to upper level easterly winds intensify and favor deep convection and westward moisture transport (Garreaud et al., 2003; Vuille and Keimig, 2004).

Precipitation in the central Peruvian Andes is sourced from the Amazon Basin (and ultimately the tropical Atlantic), by prevailing easterly winds during the austral summer. It is also during the austral summer that the Peruvian Andes receive their greatest rainfall because of increased westward moisture transport (Garreaud et al., 2003). About 60% of mean annual rainfall in the central Andes occurs during the December–March (DJFM) rainy season (Peruvian Meteorological Service, SENAMHI, unpublished data, 1919–1999). Although the seasonal temperature variation is small, the DJFM rainy season is also the warm time of the year. Average summer temperatures in the central Peruvian Andes at 3750 m are 11 °C compared to winter temperatures of 9 °C at the same elevation (SENAMHI).

Over modern interannual timescales, a primary influence on SASM intensity and precipitation amount are sea surface temperatures in the Pacific. Modern observations (Garreaud et al., 2003), proxy data (Bradley et al., 2003), and model simulations (Vuille et al., 2003) all suggest that El Niño years are typically dry and La Niña years are wet. The El Niño/dry and La Niña/wet relationship is related to the intensity and direction of the upper level winds, similar to the mechanism leading to seasonal rainfall variability. Atmospheric zonal circulation is intensified during La Niña conditions, thus supporting stronger upper level easterly winds that allow for enhanced near-surface moisture transport to the Peruvian Andes (Garreaud et al., 2003). During El Niño events, the combination of weaker easterly and enhanced westerly winds inhibits moisture transport from the Amazon Basin.

Over decadal timescales, Atlantic sea surface temperatures also play an important role on precipitation variability for tropical South America. Cold sea surface temperature anomalies and increased easterly winds from the equatorial North Atlantic are associated with precipitation increases over the continent, south of the equator (Nobre and Shukla, 1996). Model data demonstrate a relationship where North Atlantic cold phases are linked with displacement of the ITCZ away from the hemisphere with added ice cover (Chiang and Bitz, 2005). For conditions that favor increased ice cover over Greenland, the ITCZ shifts southward as a result of an enhanced subsidence of the northern branch of the Hadley Cell and increased uplift in the southern branch. Paleoclimate proxy records from the tropical Andes support this connection: precipitation increases in southern tropical South America are synchronous with North Atlantic cold events over millennial timescales (Baker et al., 2001). Precipitation decreases in northern tropical South America also occur in conjunction with North Atlantic cold phases (Haug et al., 2001). Since the ITCZ is the essential moisture conduit for the precipitation over the South American continent, the strengthening of easterly winds south of the equator could provide the mechanism for increased moisture transport across the continent during North Atlantic cool phases.

3. Materials and methods

This study uses two speleothems (P00-H1 and P09-H2) collected from Huagapo Cave (11.27°S; 75.79°W) set ~3850 m above sea level (masl) in the central Peruvian Andes. Huagapo Cave is 2800 m in length and was formed within a Triassic dolomitic limestone massif (Cobbing et al., 1981). A stream flows along the floor of the cave throughout the year, and supports an environment where relative humidity approaches 100% far from the cave entrance. The measured relative humidity of the cave environment in 2009 was greater than 95%. Late 20th century (1943–1998) mean annual external air temperatures at a meteorological station located 30 km southwest from Huagapo Cave were 10.4 ± 0.8 °C (1σ) (SENAMHI). Interannual variability of internal air temperature at Huagapo Cave is expected to be smaller than for external air

temperature. The measured internal cave air temperatures during 2000 and 2009 were 12 °C, which was within 2σ of the 1943–1998 average and within 1σ of the 1989–1998 range. The remote location of the cave precluded long-term monitoring of the cave temperature and relative humidity. P00-H1 and P09-H2 stalagmites are calcite samples that are 12 and 61 cm tall, respectively. Both samples were collected in the cave's main gallery, located approximately 650 m from the main entrance. Sample P00-H1 was collected in June 2000 and was actively growing at the time of collection. Sample P09-H2 was collected in June 2009.

Chronologies were established using a multi-collector, inductively coupled plasma mass spectrometry (MC-ICPMS) on a Thermo-Finnigan Neptune at the Minnesota Isotope Laboratory with procedures similar to those described in Cheng et al. (2009). The speleothem samples were halved along the growth axis and subsampled along growth layers for radiometric dating. Five and twenty-one ^{230}Th age determinations weighing between 80 and 160 mg were used to establish the age models for P00-H1 and P09-PH2, respectively (Table 1).

The stable oxygen and carbon isotope long-axis profiles are based on 309 measurements (P00-H1) and 1084 measurements (P09-H2) and were performed at the University of Massachusetts. Samples for stable isotope measurements were microdrilled from a cut and polished slab every 0.1–1.0 mm, permitting sub-decadal resolution throughout the record (Table 2). The samples were analyzed in an on-line carbonate preparation system linked to a Finnigan Delta Plus XL ratio mass spectrometer. Results are reported as the per mil difference between the sample and the Vienna Pee Dee Belemnite standard in delta notation where $\delta^{18}O = (R_{sample}/R_{standard} - 1)^{*}1000$, and R is the ratio of the minor to the major isotope. Reproducibility of the standard materials is 0.1‰.

Table 2
Sampling resolution of P00-H1 and P09-H2.

Sample name	Sampling interval (mm)	Depth (mm)	Average resolution (years)
P00-H1	0.2	0–65.8	4.5
P09-H2	0.5	0–10.0	3.75
P09-H2	0.1	10.0–46.8	1.4
P09-H2	0.5	46.8–224.8	3.6
P09-H2	1.0	224.8–607.8	10.4

4. Results

4.1. Age model

The combined age range for P00-H1 and P09-H2 is −50 to 7150 years before present [(BP), present = 1950] (Fig. 1). All dates for each sample are in stratigraphic order and contain high initial uranium and low detrital thorium concentrations that yield precise age determinations with low measurement errors, ±2 to ±15 years (2σ) over the entire record (Table 1). A shift in the growth axis was observed in sample P09-H2 at about 43 cm. Age measurements, taken as close as possible to the growth axis shift, did not significantly deviate from the long-term growth trend. Age models for each sample were established using linear interpolation between adjacent ^{230}Th dates.

4.2. Equilibrium versus kinetic fractionation

Stable oxygen and carbon isotope ratios ($\delta^{18}O$ and $\delta^{13}C$) were measured at an average 5-year resolution. We observe that $\delta^{18}O$

Table 1
^{230}Th dating results for (A) P00-H1 and (B) P09-H2. The error is 2σ error.

Sample no.	Depth (mm)	^{238}U (ppb)	^{232}Th (ppt)	^{230}Th/^{232}Th (atomic × 10^{-6})	$\delta^{234}U$[a] (measured)	^{230}Th/^{238}U (activity)	^{230}Th age (yr) (uncorrected)	$\delta^{234}U_{Initial}$[b] (corrected)	^{230}Th age (yr BP)[c] (corrected)
A)									
1	8.5	1143 ± 1	131 ± 3	1120 ± 30	3415 ± 4	0.0078 ± 0.0001	193 ± 2	3417 ± 4	132 ± 2
2	19	985 ± 2	642 ± 13	510 ± 10	3488 ± 6	0.0200 ± 0.0001	487 ± 3	3493 ± 6	423 ± 4
3	41.5	979 ± 1	137 ± 3	4670 ± 100	3498 ± 5	0.0396 ± 0.0001	962 ± 3	3507 ± 5	902 ± 4
4	66.5	786 ± 1	258 ± 5	2960 ± 60	3406 ± 5	0.0590 ± 0.0002	1467 ± 5	3420 ± 5	1405 ± 6
5	118.5	967 ± 2	321 ± 7	4680 ± 100	3516 ± 5	0.0941 ± 0.0002	2290 ± 6	3539 ± 5	2228 ± 6
B)									
1	5	1523 ± 2	100 ± 2	7920 ± 200	1894 ± 3	0.0316 ± 0.0001	1198 ± 4	1900 ± 3	1137 ± 4
2	13.5	1256 ± 2	22 ± 1	30,740 ± 1800	1897 ± 3	0.0333 ± 0.0001	1261 ± 4	1904 ± 3	1201 ± 4
3	21	1476 ± 2	30 ± 1	29,050 ± 1200	1914 ± 3	0.0356 ± 0.0001	1339 ± 4	1921 ± 3	1279 ± 4
4	27	918 ± 1	65 ± 2	8880 ± 230	1897 ± 3	0.0381 ± 0.0001	1442 ± 5	1904 ± 3	1381 ± 5
5	35	1068 ± 1	16 ± 1	46,680 ± 3530	1895 ± 3	0.0413 ± 0.0001	1566 ± 5	1903 ± 3	1505 ± 5
6	46	1198 ± 2	25 ± 1	36,100 ± 1540	1892 ± 3	0.0460 ± 0.0001	1745 ± 5	1902 ± 3	1685 ± 5
7	75	1283 ± 2	29 ± 1	40,040 ± 1740	1895 ± 3	0.0555 ± 0.0001	2105 ± 5	1907 ± 3	2045 ± 5
8	120	1314 ± 2	69 ± 2	20,840 ± 540	1849 ± 3	0.0661 ± 0.0001	2554 ± 6	1862 ± 3	2493 ± 6
9	178	1571 ± 2	83 ± 2	24,610 ± 600	1806 ± 3	0.0789 ± 0.0002	3100 ± 8	1822 ± 3	3040 ± 8
10	269	1924 ± 3	67 ± 2	46,120 ± 1170	1821 ± 3	0.0976 ± 0.0002	3824 ± 9	1841 ± 3	3764 ± 9
11	327	2551 ± 4	43 ± 1	108,980 ± 3620	1831 ± 3	0.1116 ± 0.0002	4368 ± 10	1854 ± 3	4308 ± 10
12	372	2536 ± 4	34 ± 1	144,010 ± 4990	1823 ± 3	0.1186 ± 0.0002	4658 ± 11	1847 ± 3	4598 ± 11
13	420	2199 ± 3	35 ± 1	137,780 ± 5060	1896 ± 3	0.1318 ± 0.0003	5057 ± 11	1923 ± 3	4997 ± 11
14	434	1360 ± 2	88 ± 2	34,420 ± 800	1870 ± 3	0.1352 ± 0.0002	5234 ± 11	1898 ± 3	5173 ± 11
15	497	1261 ± 2	24 ± 1	133,820 ± 4870	1909 ± 3	0.1561 ± 0.0003	5982 ± 12	1941 ± 3	5922 ± 12
16	539	1203 ± 1	27 ± 1	128,220 ± 5250	1972 ± 3	0.1728 ± 0.0003	6491 ± 13	2008 ± 3	6431 ± 13
17	553	1449 ± 2	24 ± 1	175,950 ± 8230	2004 ± 3	0.1801 ± 0.0003	6700 ± 14	2042 ± 3	6640 ± 14
18	563	1339 ± 2	18 ± 1	219,740 ± 11,400	1933 ± 3	0.1779 ± 0.0003	6780 ± 14	1971 ± 3	6719 ± 14
19	573	1559 ± 2	19 ± 1	247,190 ± 11650	1934 ± 3	0.1811 ± 0.0003	6900 ± 15	1972 ± 3	6840 ± 15
20	587	1608 ± 2	20 ± 1	239,640 ± 11,270	1937 ± 3	0.1842 ± 0.0003	7016 ± 13	1976 ± 3	6956 ± 13
21	604	1582 ± 2	33 ± 1	147,690 ± 5590	1948 ± 3	0.1889 ± 0.0003	7171 ± 14	1988 ± 3	7111 ± 14

Corrected ^{230}Th ages assume the initial ^{230}Th/^{232}Th atomic ratio of 4.4 ± 2.2 × 10^{-6}. Those are the values for a material at secular equilibrium, with the bulk earth ^{232}Th/^{238}U value of 3.8. The errors are arbitrarily assumed to be 50%.

[a] $\delta^{234}U = ([^{234}U/^{238}U]\text{activity} - 1)1000$.

[b] $\delta^{234}U_{initial}$ was calculated based on ^{230}Th age (T), i.e., $\delta^{234}U_{initial} = \delta^{234}U_{measured}\, e^{\lambda^{234}T}$.

[c] B.P. stands for "Before Present" where the "Present" is defined as the year 1950 A.D.

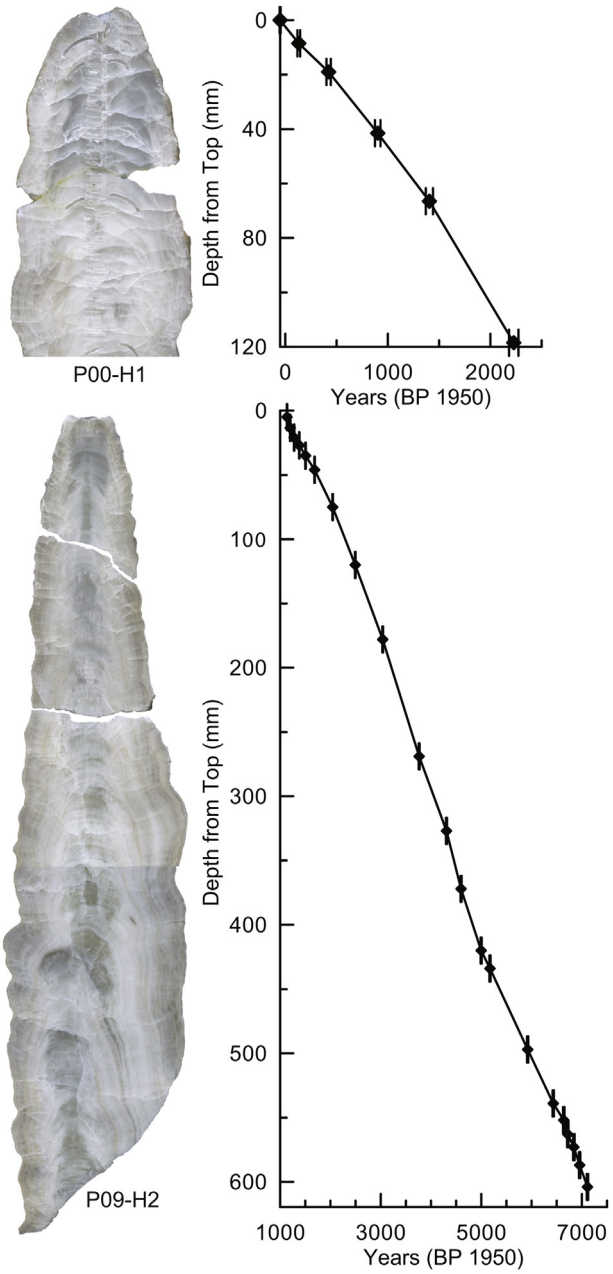

Fig. 1. Image of stalagmites P00-H1 and P09-H2 with corresponding age model. Individual age determinations are shown with errors (2σ). The age model was determined by linear interpolation between adjacent ^{230}Th dates.

and $\delta^{13}C$ are significantly correlated along the growth axis (not shown, $r^2 = 0.46$, $p < 0.05$). Even though correlation between $\delta^{18}O$ and $\delta^{13}C$ along the growth axis could indicate non-equilibrium calcite precipitation (Hendy, 1971), such covariance may also result from climatic changes affecting both isotopes (Dorale and Liu, 2009). We incorporate a second assessment to evaluate the role of kinetic effects on $\delta^{18}O$. Using the two independent age models and at different sampling resolutions, P00-H1 $\delta^{18}O$ and P09-H2 $\delta^{18}O$ compare well over multidecadal timescales for the overlapping 300-year growth interval (1.1–1.4 ka) (Fig. 2A–C). From 1100 to 1400 years ago, the two oxygen isotope records are nearly identical both in terms of the mean values and the magnitude of change (i.e. no offset is applied to shift the time series of one stalagmite in order to match the other) even though the speleothems have different sampling resolutions and age models (Fig. 2B). Specifically, the difference in mean $\delta^{18}O$ values of P00-H1 and P09-H2 at 50-year intervals during the overlapping period is always equal to or less than 0.1‰, the measurement uncertainty (Fig. 2C). In addition, both stalagmites captured the ~0.5‰ increase over this time. The small offset in the increase at 1150 years ago is likely due to sample resolution because P09-H2 was subsampled at much higher resolution compared to P00-H1 for this short interval. This replication in the $\delta^{18}O$ records of the two samples indicates that speleothem calcite is not significantly impacted by kinetic isotope effects since we would expect that such effects would be sample specific (Hendy, 1971). The oxygen isotope replication analysis and comparison to other nearby paleoclimate records, described below, suggests that most of the $\delta^{18}O$ variability is likely due to climatic factors at decadal timescales and longer. Thus, the two records were combined using P09-H2 as the primary sample and P00-H1 to extend the record to modern time. We cannot rule out, however, that sub-decadal variations could, in part, be due to non-climatic factors and thus climatic interpretations are considered for decadal timescales and longer only.

4.3. Oxygen isotopic variability

Huagapo Cave $\delta^{18}O$ ranges from −14‰ to −12‰ between −50 and 7150 years BP and exhibits significant variance over decadal to millennial timescales (Fig. 2A). A gradual decrease of 2‰ from the mid-Holocene to the modern era is punctuated by centennial-scale deviations during the late Holocene. The most prominent characteristic is a gradual 1.5‰ rise that has a peak of −12.5‰ at 1.5 ka. This deviation from the long-term trend is near symmetrical in shape and the full excursion occurs over two millennia. Two more rapid increases in $\delta^{18}O$, one at 2.6 ka and another at ~250 yr BP, occurred over a few centuries or less and are defined by local isotopic maxima of about −12‰. Higher frequency changes, which have amplitudes of slightly less than 1‰ and occur over timescales of a few decades, characterize the entire record.

5. Discussion

5.1. Climatic influences on speleothem oxygen isotopes

A variety of factors might influence rainfall $\delta^{18}O$ at the cave site, including moisture source variability, isotopic composition of the moisture source, condensation temperature, and rainfall amount effects both local and upstream. Of these factors, the moisture source and its $\delta^{18}O$ value, and temperature are unlikely to be an important influence on Huagapo Cave $\delta^{18}O_{calcite}$ for the Holocene. The tropical Atlantic is the sole moisture source for the SASM and the estimated change in the seawater $\delta^{18}O$ due to melting of Pleistocene ice sheets for the last 5000 years is only about −0.1‰ (Fairbanks, 1989; Polissar et al., 2006), an amount that is within measurement uncertainty. With respect to temperature, the observed 2‰ decrease in Huagapo Cave $\delta^{18}O_{calcite}$ would require a local 8 °C warming, based on the calcite–water equilibrium isotope fractionation (Kim and O'Neil, 1997). A change of this magnitude is unreasonably large for the Holocene, where the estimated temperature change at the transition out of the Last Glacial Maximum and into the Holocene is 3 °C (Pierrehumbert, 1999). Over centennial scales, temperature is also unlikely to be the primary influence because, for example, during the LIA the observed isotope values are the lightest values of the entire record. If regional cooling occurred during the LIA, as it did in the Northern Hemisphere, the isotope values should be heavier due to an increase in the water-calcite fractionation at lower

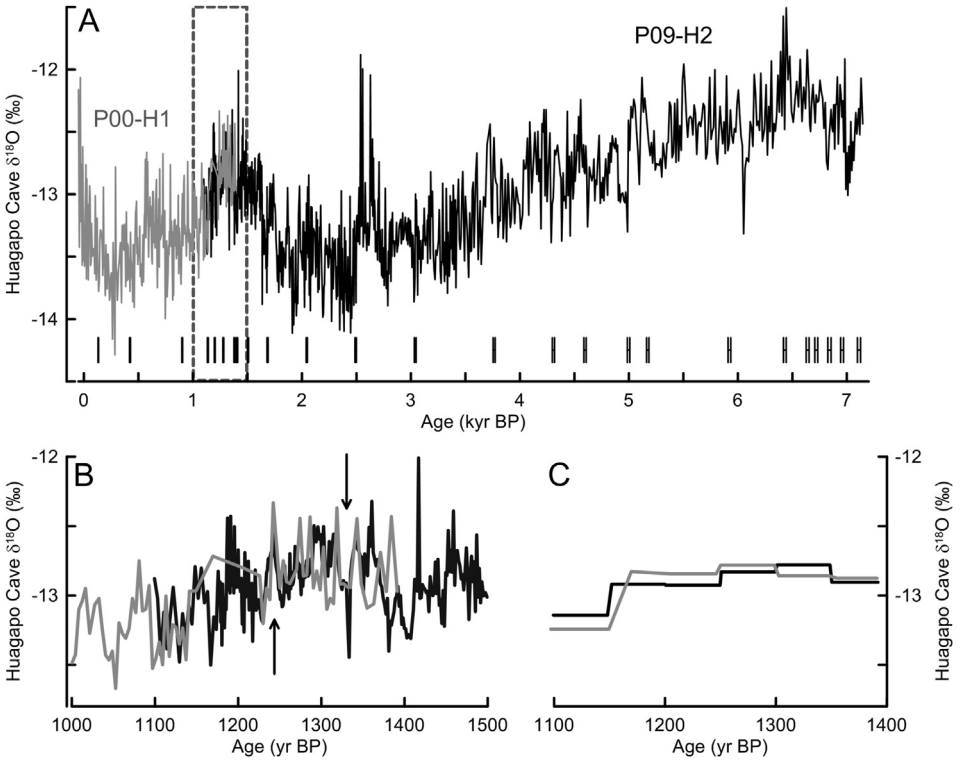

Fig. 2. (A) Time series of P00-H1 (gray) and P09-H2 (black) $\delta^{18}O$ subsampled along the growth axis. U/Th dates with 2σ uncertainty bars are shown. Dashed box indicates the interval of overlap between the two stalagmites. (B) Inter-sample comparison between P00-H1 (gray) and P09-H2 (black) for Huagapo Cave $\delta^{18}O$ for the overlapping time interval. Arrows indicate decadal-scale agreement between the two samples. (C) Comparison of the 50-year averages in $\delta^{18}O$ for P00-H1 and P09-H2. The difference in the mean values between the two samples is always equal to or less than 0.1‰.

temperatures. Thus, centennial-scale temperature changes of the last two millennia would act in a way to dampen, rather than enhance the isotopic variability. Late 20th century meteorological data indicate that external air temperature varied by at most 1 °C on sub-decadal timescales, which would cause 0.25‰ variation in $\delta^{18}O$. In addition, variability of internal cave temperature is likely to be less.

Instead, modern observations and model simulations indicate that precipitation amount is the primary control on rainfall $\delta^{18}O$ in tropical South America over short and long timescales. For seasonal timescales, simulated monthly rainfall $\delta^{18}O$ minima coincide with the DJF rainy season in the central Peruvian Andes (Vuille et al., 2003). Over interannual timescales, precipitation $\delta^{18}O$ in the Amazon Basin is closely correlated to the intensity of the SASM, where a stronger SASM leads to more depleted values in precipitation $\delta^{18}O$ (Vuille and Werner, 2005). A negative correlation between precipitation amount and $\delta^{18}O$ over seasonal and interannual timescales is consistent with the so-called 'amount effect' where enhanced convection and increased precipitation is associated with more negative $\delta^{18}O$ via a Rayleigh-type fractionation and a number of other associated effects (Dansgaard, 1964; Rozanski et al., 1993; Lee and Fung, 2008; Risi et al., 2008).

Interannual SASM intensity is not only a primary influence on the climatology of the Amazon Basin but also on Andean precipitation amount and $\delta^{18}O$. In a 20-year simulation (1979–1998), model simulations from ECHAM4 demonstrated that the isotopic signal of the monsoon is preserved and enhanced along the moisture path from eastern Amazonia to the Peruvian Andes (Vuille and Werner, 2005). The importance of upstream rainout was further demonstrated using a combined proxy reconstruction of the 20th century from four tropical Andean ice cores (Hoffmann et al., 2003) and in a 92-year ECHAM4 simulation for the Bolivian Andes (Vimeux et al., 2005). Thus, the isotopic composition of rainfall in the Andes integrates the effects of rainout of the heavy isotope along the moisture transport pathway.

The correlation between interannual central Andean $\delta^{18}O$ and ENSO has also been demonstrated using model and proxy data for the last several decades (Bradley et al., 2003; Vuille and Werner, 2005). Specifically, La Niña years are associated with increased precipitation upstream, enhanced moisture transport, and lighter rainfall $\delta^{18}O$ (Garreaud et al., 2003). Atmospheric climatic conditions are essentially reversed during El Niño episodes and Andean rainfall $\delta^{18}O$ is typically heavier during ENSO warm phases. Thus, we interpret the primary changes in $\delta^{18}O_{calcite}$ to be driven by the isotopic composition of precipitation at the study site, which itself is largely influenced by the intensity of the SASM via upstream rainout.

5.2. Orbital-scale climatic changes

The long-term trend of Huagapo Cave $\delta^{18}O$ resembles other cave, ice core, and lake sediment Holocene records from the tropical Peruvian Andes. A map of the locations of the Peruvian climate reconstructions discussed in the text is shown in Fig. 3 and the associated time series are shown in Figs. 4–6. To evaluate regional consistency and the role of upstream changes, we compare ice core and cave records that span 4500 m in elevation and are as much as 650 km apart. The high elevation reconstruction from Huascarán ice core $\delta^{18}O$ (9°6'S 77°36'W, 6048 masl) (Thompson et al., 1995) shows a trend from the mid to late Holocene that is of the same magnitude and direction, Δ2‰/7 ka, as Huagapo Cave $\delta^{18}O$ (Fig. 4A). We note that Huascarán $\delta^{18}O_{ice}$ was originally interpreted as proxy for paleo-temperatures (Thompson et al., 1995), but other explanations of the tropical Andean ice core records suggest that

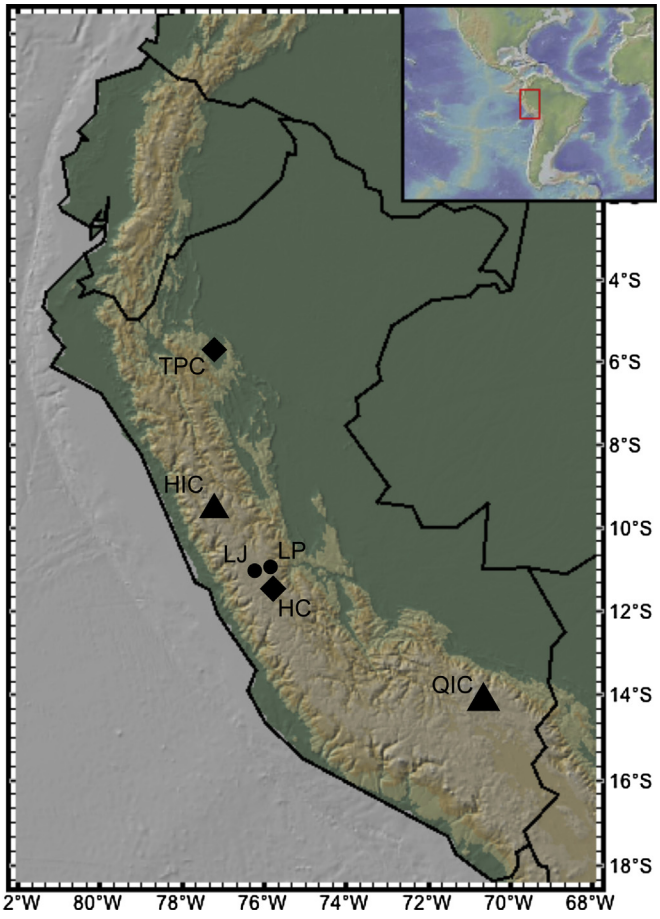

Fig. 3. Map of Peru showing the locations of the paleoclimate records discussed in the text (TPC, Cueva del Tigre Perdido; HIC, Huascarán Ice Cap; LJ, Lake Junin; LP, Laguna Pumacocha; HC, Huagapo Cave; QIC, Quelccaya Ice Cap).

precipitation amount and degree of ^{18}O rainout upstream is the primary influence (Hoffmann et al., 2003; Hastenrath et al., 2004). Similar, mean-state $\delta^{18}O$ changes are also observed at the lowest elevation site, Cueva del Tigre Perdido, which is located on the northeastern flank of the Peruvian Andes (5°30′S 77°W, 1400 masl) (vanBreukelen et al., 2008) (Fig. 4B). Shared long-term variance of the three records (Huascarán, Cueva del Tigre Perdido, and Huagapo Cave) over large differences in elevation supports the interpretation of vanBreukelen et al. (2008) that the vertical temperature gradient (lapse rate) remained constant through the Holocene. The commonality of these records also points toward a shared upstream moisture source, the SASM, which intensified from the mid to late Holocene.

Strengthening of the SASM into the late Holocene, however, may also be accompanied by an intensification of more local rainfall in the central Peruvian Andes based on comparison to nearby lake sediment reconstructions. The oxygen isotopic composition of lake sediments represents surface water conditions, specifically precipitation minus evaporation. Direct comparison of cave (or ice core) and lake sediment reconstructions can clarify the evaporation history of the region. Lake Junin (4000 masl) is situated only 30 km northwest from Huagapo Cave and is the paleoclimate record that is most proximate to the study site (Seltzer et al., 2000) (Fig. 4C). The change in $\delta^{18}O$ over the last seven thousand years is three times greater in magnitude for the lake compared to the cave ($\Delta\delta_{Junin}$: 6‰; $\Delta\delta_{Huagapo}$: 2‰). In other words, if the observed $\delta^{18}O$ difference between Lake Junin and Huagapo Cave over the mid to late Holocene is real, it indicates a decrease in evaporative enrichment and overall wetter conditions, consistent with the original Lake Junin interpretation (Seltzer et al., 2000). A similar assessment can also be obtained by comparison to a recent reconstruction from a high-elevation carbonate lake, Laguna Pumacocha (10°42′S 76°W, 4300 masl) (Bird et al., 2011a, 2011b) (Fig. 4D). In this comparison, mean-state trends in Pumacocha authigenic calcite $\delta^{18}O$ are about twice as large as Huagapo Cave through the Holocene ($\Delta\delta_{Pumacocha}$: 4‰). A smaller $\Delta\delta$ for Laguna Pumacocha compared to Lake Junin may be reasonable because precipitation $\delta^{18}O$ rather than surface water evaporative enrichment is the primary influence on authigenic calcite $\delta^{18}O$ for Laguna Pumacocha (Bird et al., 2011a). All combined, these five records likely indicate a synchronous history of climatic change over the last seven millennia that may have been dominated by precipitation increases locally and a strengthening of the SASM upstream.

The observed long-term trend in tropical South American climate through the Holocene appears to be influenced by SASM intensity, which itself may be linked to seasonal changes in insolation (Fig. 4E). A comparison between austral summer insolation and the Andean climate records described indicates that over orbital timescales increased local summer insolation is correlated with enhanced SASM precipitation in southern tropical South America. Solar insolation is well established as the primary forcing mechanism for changes in monsoon intensity in the northern and southern hemispheres for Holocene and Late Pleistocene reconstructions (Cruz et al., 2005; Wang et al., 2008). Mechanistically, higher summer solar insolation can lead to greater sensible heating of the continent, increased atmospheric convection and enhanced monsoon rainfall.

Over the Holocene, mean-state changes in ENSO have also been proposed. Paleoclimate reconstructions from the eastern (Moy et al., 2002; Rein et al., 2005; Conroy et al., 2008) and western equatorial Pacific (Gagan et al., 2004) suggest that El Niño activity may have been reduced in the early and mid-Holocene compared to today. Model simulations support that ENSO variance could have increased in the Late Holocene when tropical seasonality was reduced and the ITCZ shifted southward (Clement et al., 2000). Yet if these changes in El Niño frequency and amplitude were a primary influence on our record, we would expect to see the opposite long-term trend from what is observed. An increase in El Niño-like conditions would be expected to generate a shift to heavier rather than lighter isotope values in the Late Holocene. Our record from Huagapo Cave, and others from the Peruvian Andes, suggest that on orbital timescales changes in ENSO frequency and/or amplitude may be subordinate to insolation changes in the tropics, despite of the dominance of ENSO in recent inter-annual records.

Meridional sea surface temperature gradients, as characterized by latitudinal shifts in the ITCZ, are also important to modern precipitation variability in tropical South America and likely have an important role over the Holocene as well. The relative position of the Holocene ITCZ has been interpreted from changes in titanium concentrations from Cariaco Basin sediment cores off the coast of Venezuela (Haug et al., 2001) and the Huagapo Cave record also resembles inferred ITCZ variance, which itself tracks insolation changes over orbital timescales (Fig. 4F). In general, an increase (reduction) in summertime rainfall and surface runoff in the Cariaco Basin, located in the northern tropical Atlantic (Haug et al., 2001) is linked with decreased (increased) SASM intensity. The relation between ITCZ position and SASM intensity suggests that the two could be mechanistically related over orbital timescales. When the ITCZ is displaced southward, warmer sea surface temperatures in the southern equatorial Atlantic and enhanced easterly winds could transport more moisture onto the continent and intensify the monsoon. However, the records are decoupled for

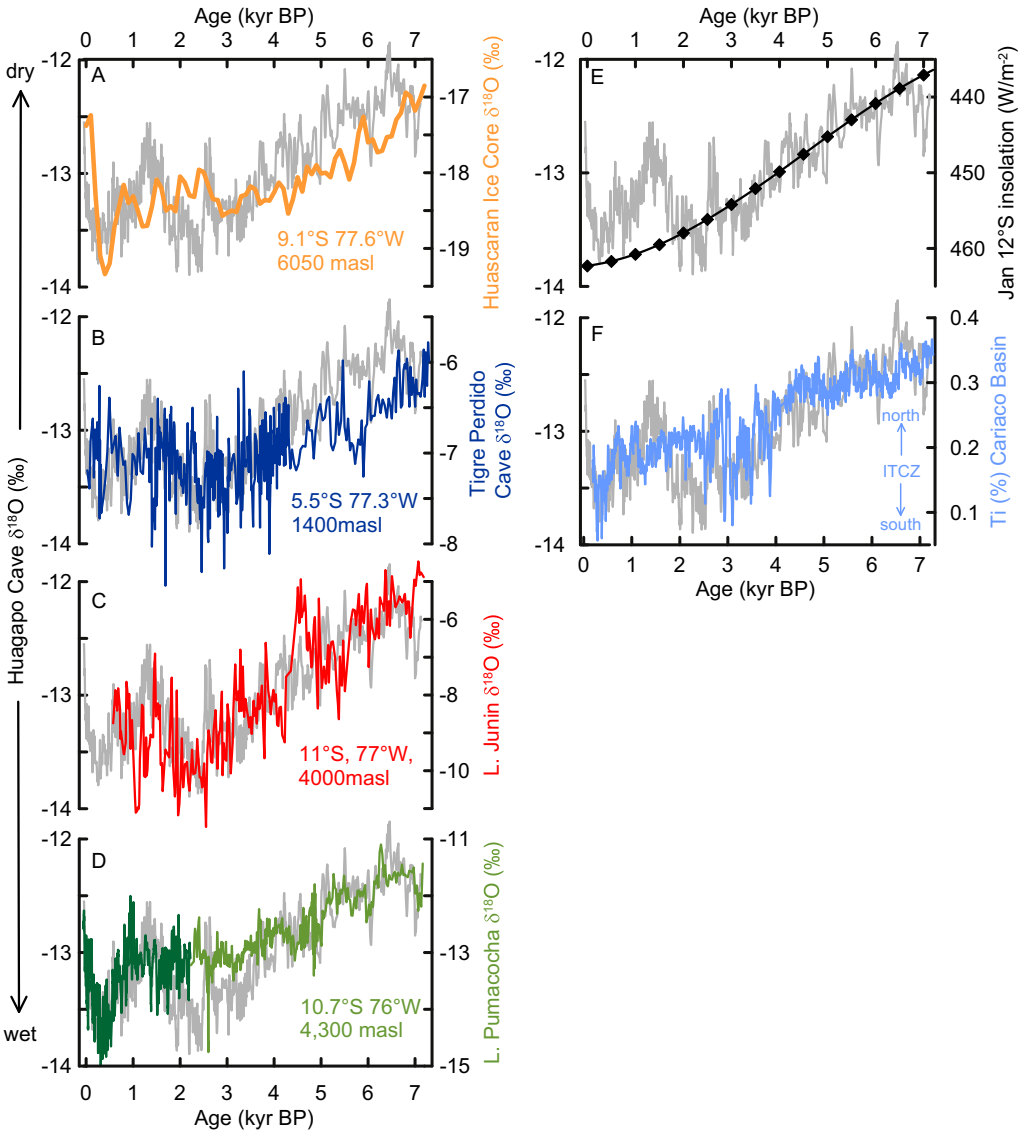

Fig. 4. Huagapo Cave $\delta^{18}O$ record of SASM intensity in comparison with Andean Holocene climate reconstructions. (Left Panel) In A through D, the Huagapo Cave $\delta^{18}O$ time series is shown as a 3-pt smooth, 5-year resample (gray). (A) Huascarán ice core $\delta^{18}O$ (orange) (Thompson et al., 1995), (B) Cueva del Tigre Perdido stalagmite $\delta^{18}O$ (blue) (vanBreukelen et al., 2008), (C) Lake Junin authigenic calcite $\delta^{18}O$ (red) (Seltzer et al., 2000), (D) Laguna Pumacocha varved record [dark green, 7-pt running average (Bird et al., 2011b)] and Holocene record [light green (Bird et al., 2011a)] of authigenic calcite $\delta^{18}O$. (Right Panel) Huagapo Cave $\delta^{18}O$ time series is shown in comparison to (E) January insolation at 12°S (black) (Laskar et al., 2004), and (F) titanium content from the Cariaco Basin (light blue) (Haug et al., 2001). (For interpretation of the references to color in this figure legend, the reader is referred to the web version of this article.)

periods in the Late Holocene and specifically between 1 and 3 ka, indicating that other influences may be operative on sub-orbital timescales.

5.3. Millennial to centennial scale variability

Centennial-scale variance in the Late Holocene (<3000 years ago) is an important characteristic of the Huagapo Cave record because the isotopic data are partially decoupled from the ITCZ proxy and deviate from the insolation curve. The most prominent characteristic is a gradual 1.5‰ rise that has a peak of −12.5‰ at 1500 years ago and a second feature is another increase in the isotope values, which begins at about 250 years ago and continues into the modern era. These shifts to higher values in speleothem $\delta^{18}O$ indicate that a forcing mechanism other than insolation, which was approaching a local maximum, might have caused SASM intensity to decrease in the Late Holocene. We investigate the influence of the tropical Pacific at sub-orbital timescales over the last few millennia.

Although at lower resolution than the terrestrial records, there are similar variations between equatorial Pacific SST reconstructions and the Huagapo Cave record for the last several thousand years (Stott et al., 2004; Rein et al., 2005) (Fig. 5). In the eastern and western portions of the basin (Fig. 5A and B), a warm interval of a few degrees Celsius in the late Holocene is coincident with higher values in Huagapo Cave $\delta^{18}O$ and an inferred decrease in SASM intensity. Furthermore, the zonal SST gradient, calculated as the difference between the western (Stott et al., 2004) and eastern (Rein et al., 2005) SST reconstructions, also shows similar millennial-scale trends to the Huagapo Cave record, specifically for the last 3000 years. A weaker (stronger) zonal SST gradient, and presumably weaker Walker circulation, could be linked with

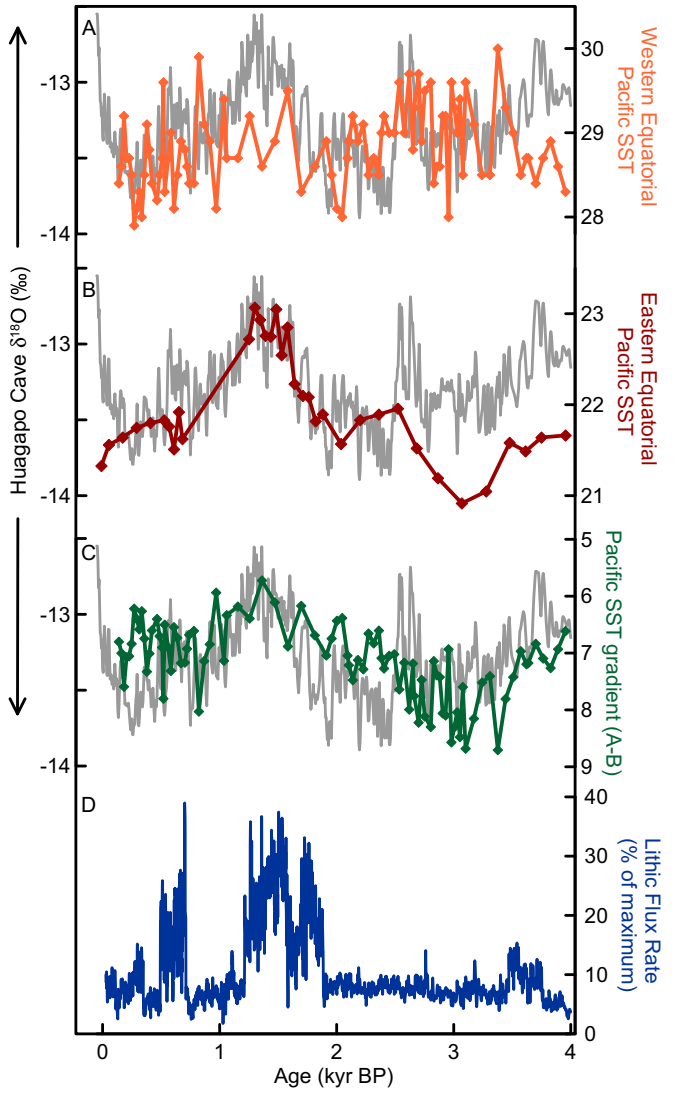

Fig. 5. Holocene sea surface temperature reconstructions from the tropical Pacific Ocean. In A through C, the Huagapo Cave $\delta^{18}O$ time series is shown as a 3-pt smooth, 5-year resample. (A) Mg/Ca-derived SST reconstruction from the western equatorial Pacific (Stott et al., 2004), (B) alkenone-based SST reconstruction off the Peruvian coast (Rein et al., 2005), and (C) Zonal SST gradient for the tropical Pacific calculated as the difference between (A) and (B). (D) Paleo-ENSO lithic flux reconstruction off the coast of central Peru (Rein et al., 2005).

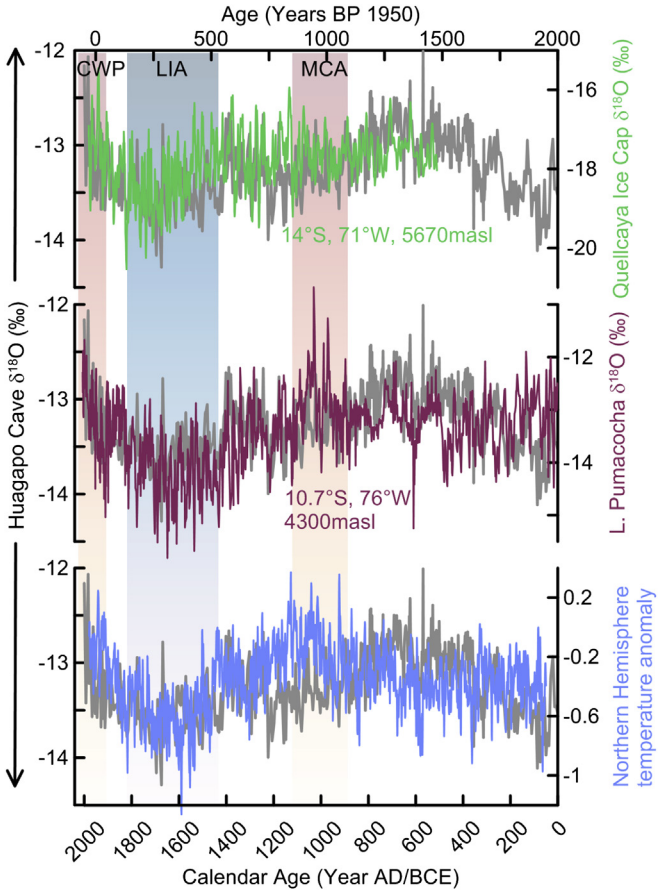

Fig. 6. High-resolution climate reconstructions from the central Peruvian Andes for the Late Holocene. Huagapo Cave $\delta^{18}O$ are shown in gray with (top) Quelccaya Ice Cap $\delta^{18}O$ (green, 9-pt running average) (Thompson et al., 1986), (middle) Laguna Pumacocha authigenic calcite $\delta^{18}O$ (purple, 5-pt running average) (Bird et al., 2011b), and (bottom) Northern Hemisphere temperature anomalies (Moberg et al., 2005). (For interpretation of the references to color in this figure legend, the reader is referred to the web version of this article.)

decreased (increased) precipitation. In the modern era, positive SST anomalies in the eastern equatorial Pacific and a reduced zonal SST gradient are associated with rainfall decline in the Amazon Basin and higher precipitation $\delta^{18}O$ and reduced precipitation in the Peruvian Andes (Garreaud et al., 2003; Vuille and Werner, 2005; Garreaud et al., 2009).

The nature or causes of the shifts in the Late Holocene may also be related to the onset of modern ENSO variability as suggested by terrestrial precipitation proxy records from the eastern equatorial Pacific (Fig. 5D). Several reconstructions of climate variability in this region seem to indicate a rise in the intensity and frequency of El Niño-like events over the last 2–3 thousand years. Specifically, surface runoff records from western Ecuador (Moy et al., 2002), the Peruvian coast (Rein et al., 2005), and the Galapagos (Conroy et al., 2008) indicate two intervals (500–750 and 1500–2000 years ago) of increased precipitation during the late Holocene. The Huagapo Cave record also demonstrates two similarly timed intervals of higher isotope ratios and inferred reduced precipitation. A weaker monsoon and reduced transport of moisture up into the Peruvian Andes resembles modern-day El Niño conditions (Garreaud et al., 2003, 2009).

Consistent with the conclusions of Vuille et al. (2012), Huagapo Cave $\delta^{18}O$ is well correlated with other high resolution SASM records during the MCA, LIA, and CWP (Fig. 6). The SASM may have strengthened during the North Atlantic cold interval of the LIA and weakened during the warm intervals of the MCA and CWP. In this scenario, centennial-scale variance would be primarily influenced by North Atlantic climate variability and the meridional gradient in the tropical Atlantic Ocean rather than ENSO-related zonal circulation over the Pacific Ocean. Thus, over the last few millennia, tropical South American climate variance may result from the interplay between Northern Hemisphere temperatures, which may be important over 100-year timescales, and the zonal SST gradient in the tropical Pacific that might be operative over 1000-year timescales.

Finally, the highest resolution intervals from Quelccaya Ice Cap and Laguna Pumacocha do not extend beyond the last two millennia at similar interannual timescales. For Huagapo Cave, the centennial-scale changes in SASM intensity in the Late Holocene represent neither the wettest or driest intervals of the last 7150 years. For example, the light isotope values during the LIA are similar to values that were reached during an older interval of time

between 2000 and 2500 years ago, just prior to the deviation from the insolation forcing. Similarly, the dry interval of the MCA was not as dry as the mid-Holocene (5–7 ka) or other periods in the Late Holocene, including the CWP and between 1100 and 1500 years ago. While Northern Hemisphere temperature could be an important driver of tropical South American climate in the Late Holocene, its influence is difficult to assess because there are few temperature reconstructions that extend beyond the last 2000 years at decadal timescales.

6. Conclusions

Variations in Huagapo Cave $\delta^{18}O_c$ from the mid Holocene to the modern era contain a record of changes in local precipitation and upstream SASM intensity. In agreement with other central Andean paleoclimate records, long-term mean state changes over the last 7150 years show a correlation to austral summer insolation where an increase in local summer insolation may be linked with increased local and upstream precipitation as well as enhanced SASM intensity. Significant deviations from the long-term trend occur in the Late Holocene as indicated by higher $\delta^{18}O$ that nearly reach mid-Holocene values. This shift to heavier isotope values supports other ENSO-influenced paleoclimate records from the eastern equatorial Pacific that would indicate an increase in the frequency and intensity of El Niño events at about 1–2 ka. The Late Holocene may also be a time interval when SSTs in the equatorial Pacific warm by about 1–2 °C, likely weakening the zonal gradient in the equatorial oceans.

Acknowledgments

This work is supported by NSF grants ATM-1003466 to S.J.B., 0502535 and 1103403 to R.L.E. and H.C., NSFC 41230524 and 2013CB955902 to H.C., and AGS-1003690 to M.V. We thank C. Morales-Bermudez for his invaluable assistance in the field. Comments from two anonymous reviewers significantly helped to improve the manuscript. The data in this paper are archived online at ftp://ftp.ncdc.noaa.gov/pub/data/paleo.

Appendix A. Supplementary data

Supplementary data related to this article can be found at http://dx.doi.org/10.1016/j.quascirev.2013.05.008.

References

Abbott, M., Wolfe, B., Wolfe, A., Seltzer, G., Aravena, R., Mark, B., Polissar, P., Rodbell, D., Rowe, H., Vuille, M., 2003. Holocene paleohydrology and glacial history of the central Andes using multiproxy lake sediment studies. Palaeogeography, Palaeoclimatology, Palaeoecology 194, 123–138. http://dx.doi.org/10.1016/s0031-0182(03)00274-8.

Abbott, M.B., Seltzer, G.O., Kelts, K.R., Southon, J., 1997. Holocene paleohydrology of the tropical Andes from lake records. Quaternary Research 47, 70–80.

Baker, P.A., Rigsby, C.A., Seltzer, G.O., Fritz, S.C., Lowenstein, T.K., Bacher, N.P., Veliz, C., 2001. Tropical climate changes at millennial and orbital timescales on the Bolivian Altiplano. Nature 409, 698–701.

Bird, B.W., Abbott, M.B., Rodbell, D.T., Vuille, M., 2011a. Holocene tropical South American hydroclimate revealed from a decadally resolved lake sediment $\delta^{18}O$ record. Earth and Planetary Science Letters 310, 192–202. http://dx.doi.org/10.1016/j.epsl.2011.08.040.

Bird, B.W., Abbott, M.B., Vuille, M., Rodbell, D.T., Stansell, N.D., Rosenmeier, M.F., 2011b. A 2,300-year-long annually resolved record of the South American summer monsoon from the Peruvian Andes. Proceedings of the National Academy of Sciences of the United States of America 108, 8583–8588. http://dx.doi.org/10.1073/Pnas.1003719108.

Bradley, R.S., Vuille, M., Hardy, D., Thompson, L.G., 2003. Low latitude ice cores record Pacific sea surface temperatures. Geophysical Research Letters 30, 1174. http://dx.doi.org/10.1029/2002gl016546.

Cheng, H., Fleitmann, D., Edwards, R.L., Wang, X., Cruz, F.W., Auler, A.S., Mangini, A., Wang, Y., Kong, X., Burns, S.J., Matter, A., 2009. Timing and structure of the 8.2 kyr B.P. event inferred from ^{18}O records of stalagmites from China, Oman, and Brazil. Geology 37, 1007–1010. http://dx.doi.org/10.1130/g30126a.1.

Chiang, J.C.H., Bitz, C.M., 2005. Influence of high latitude ice cover on the marine Intertropical Convergence Zone. Climate Dynamics 25, 477–496. http://dx.doi.org/10.1007/S00382-005-0040-5.

Clement, A.C., Seager, R., Cane, M.A., 2000. Suppression of El Nino during the mid-Holocene by changes in the Earth's orbit. Paleoceanography 15, 731–737. http://dx.doi.org/10.1029/1999PA000466.

Cobbing, E.J., Pitcher, W.S., Wilson, J.J., Baldock, J.W., Taylor, W.P., McCourt, W., Snelling, N.J., 1981. The Geology of the Western Cordillera of Northern Peru. Great Britain Institute of Geological Sciences, Natural Environmental Research Council, p. 143.

Conroy, J.L., Overpeck, J.T., Cole, J.E., Shanahan, T.M., Steinitz-Kannan, M., 2008. Holocene changes in eastern tropical Pacific climate inferred from a Galapagos lake sediment record. Quaternary Science Reviews 27, 1166–1180. http://dx.doi.org/10.1016/j.quascirev.2008.02.015.

Cruz, F.W., Burns, S.J., Karmann, I., Sharp, W.D., Vuille, M., Cardoso, A.O., Ferrari, J.A., Dias, P.L.S., Viana, O., 2005. Insolation-driven changes in atmospheric circulation over the past 116,000 years in subtropical Brazil. Nature 434, 63–66. http://dx.doi.org/10.1038/Nature03365.

Dansgaard, W., 1964. Stable isotopes in precipitation. Tellus 16, 436–468.

Dorale, J.A., Liu, Z.H., 2009. Limitations of Hendy test criteria in judging the paleoclimatic suitability of speleothems and the need for replication. Journal of Cave and Karst Studies 71, 73–80.

Fairbanks, R.G., 1989. A 17,000-year glacio-eustatic sea-level record – influence of glacial melting rates on the Younger Dryas event and deep-ocean circulation. Nature 342, 637–642.

Gagan, M.K., Hendy, E.J., Haberle, S.G., Hantoro, W.S., 2004. Post-glacial evolution of the Indo-Pacific warm pool and El Nino-Southern Oscillation. Quaternary International 118, 127–143. http://dx.doi.org/10.1016/S1040-6182(03)00134-4.

Garreaud, R., Vuille, M., Clement, A., 2003. The climate of the Altiplano: observed current conditions and mechanisms of past changes. Palaeogeography, Palaeoclimatology, Palaeoecology 194, 5–22. http://dx.doi.org/10.1016/s0031-0182(03)00269-4.

Garreaud, R.D., Vuille, M., Compagnucci, R., Marengo, J., 2009. Present-day South American climate. Palaeogeography, Palaeoclimatology, Palaeoecology 281, 180–195. http://dx.doi.org/10.1016/J.Palaeo.2007.10.032.

Hastenrath, S., Polzin, D., Francou, B., 2004. Circulation variability reflected in ice core and lake records of the southern tropical Andes. Climatic Change 64, 361–375.

Haug, G.H., Hughen, K.A., Sigman, D.M., Peterson, L.C., Rohl, U., 2001. Southward migration of the intertropical convergence zone through the Holocene. Science 293, 1304–1308.

Hendy, C.H., 1971. Isotopic geochemistry of speleothems .1. Calculation of effects of different modes of formation on isotopic composition of speleothems and their applicability as palaeoclimatic indicators. Geochimica Et Cosmochimica Acta 35, 801–824.

Hoffmann, G., Ramirez, E., Taupin, J.D., Francou, B., Ribstein, P., Delmas, R., Durr, H., Gallaire, R., Simoes, J., Schotterer, U., Stievenard, M., Werner, M., 2003. Coherent isotope history of Andean ice cores over the last century. Geophysical Research Letters 30, 1178. http://dx.doi.org/10.1029/2002gl014870.

Kim, S.T., O'Neil, J.R., 1997. Equilibrium and nonequilibrium oxygen isotope effects in synthetic carbonates. Geochimica Et Cosmochimica Acta 61, 3461–3475.

Laskar, J., Robutel, P., Joutel, F., Gastineau, M., Correia, A.C.M., Levrard, B., 2004. A long-term numerical solution for the insolation quantities of the Earth. Astronomy & Astrophysics 428, 261–285. http://dx.doi.org/10.1051/0004-6361:20041335.

Lee, J.E., Fung, I., 2008. "Amount effect" of water isotopes and quantitative analysis of post-condensation processes. Hydrological Processes 22, 1–8. http://dx.doi.org/10.1002/Hyp.6637.

Lenters, J.D., Cook, K.H., 1997. On the origin of the Bolivian high and related circulation features of the South American climate. Journal of the Atmospheric Sciences 54, 656–677.

Luan, Y., Braconnot, P., Yu, Y., Zheng, W., Marti, O., 2012. Early and mid-Holocene climate in the tropical Pacific: seasonal cycle and interannual variability induced by insolation changes. Climate of the Past 8, 1093–1108. http://dx.doi.org/10.5194/cp-8-1093-2012.

Moberg, A., Sonechkin, D.M., Holmgren, K., Datsenko, N.M., Karlen, W., 2005. Highly variable Northern Hemisphere temperatures reconstructed from low- and high-resolution proxy data. Nature 433, 613–617.

Moy, C.M., Seltzer, G.O., Rodbell, D.T., Anderson, D.M., 2002. Variability of El Nino/Southern Oscillation activity at millennial timescales during the Holocene epoch. Nature 420, 162–165.

Nobre, P., Shukla, J., 1996. Variations of sea surface temperature, wind stress, and rainfall over the tropical Atlantic and South America. Journal of Climate 9, 2464–2479.

Pierrehumbert, R.T., 1999. Huascaran delta O-18 as an indicator of tropical climate during the Last Glacial Maximum. Geophysical Research Letters 26, 1345–1348.

Polissar, P.J., Abbott, M.B., Shemesh, A., Wolfe, A.P., Bradley, R.S., 2006. Holocene hydrologic balance of tropical South America from oxygen isotopes of lake sediment opal, Venezuelan Andes. Earth and Planetary Science Letters 242, 375–389. http://dx.doi.org/10.1016/j.epsl.2005.12.02.

Rein, B., Luckge, A., Reinhardt, L., Sirocko, F., Wolf, A., Dullo, W.C., 2005. El Nino variability off Peru during the last 20,000 years. Paleoceanography 20, PA4003.

Reuter, J., Stott, L., Khider, D., Sinha, A., Cheng, H., Edwards, R.L., 2009. A new perspective on the hydroclimate variability in northern South America during the Little Ice Age. Geophysical Research Letters 36, L21706.

Risi, C., Bony, S., Vimeux, F., 2008. Influence of convective processes on the isotopic composition ($\delta^{18}O$ and δD) of precipitation and water vapor in the tropics: 2. Physical interpretation of the amount effect. Journal of Geophysical Research – Atmospheres 113, D19306.

Rozanski, K., Araguas-Araguas, L., Gonfiantini, R., 1993. Isotopic patterns in modern global precipitation. In: Swart, P.K., Lohmann, K.C., McKenzie, J., Savin, S. (Eds.), Climate Change in Continental Isotopic Records. American Geophysical Union, Geophysical Monograph, vol. 78, pp. 1–36.

Seltzer, G., Rodbell, D., Burns, S., 2000. Isotopic evidence for late Quaternary climatic change in tropical South America. Geology 28, 35–38.

Seluchi, M.E., Saulo, A.C., Nicolini, M., Satyamurty, P., 2003. The northwestern Argentinean low: a study of two typical events. Monthly Weather Review 131, 2361–2378.

Smith, J.A., Rodbell, D.T., 2010. Cross-cutting moraines reveal evidence for North Atlantic influence on glaciers in the tropical Andes. Journal of Quaternary Science 25, 243–248. http://dx.doi.org/10.1002/Jqs.1393.

Stott, L., Cannariato, K., Thunell, R., Haug, G.H., Koutavas, A., Lund, S., 2004. Decline of surface temperature and salinity in the western tropical Pacific Ocean in the Holocene epoch. Nature 431, 56–59. http://dx.doi.org/10.1038/Nature02903.

Thompson, L.G., Mosley-Thompson, E., Arnao, B.M., 1984. El-Nino Southern Oscillation events recorded in the stratigraphy of the tropical Quelccaya Ice Cap, Peru. Science 226, 50–53.

Thompson, L.G., Mosley-Thompson, E., Dansgaard, W., Grootes, P.M., 1986. The Little Ice-Age as recorded in the stratigraphy of the tropical Quelccaya Ice Cap. Science 234, 361–364.

Thompson, L.G., Mosley-Thompson, E., Davis, M.E., Lin, P.N., Henderson, K.A., Cole-Dai, J., Bolzan, J.F., Liu, K.B., 1995. Lateglacial stage and Holocene tropical ice core records from Huascaran, Peru. Science 269, 46–50.

Thompson, L.G., Mosley-Thompson, E., Henderson, K.A., 2000. Ice-core palaeoclimate records in tropical South America since the Last Glacial Maximum. Journal of Quaternary Science 15, 377–394.

Thompson, L.G., Mosley-Thompson, E., Brecher, H., Davis, M., Leon, B., Les, D., Lin, P.N., Mashiotta, T., Mountain, K., 2006. Abrupt tropical climate change: past and present. Proceedings of the National Academy of Sciences of the United States of America 103, 10536–10543. http://dx.doi.org/10.1073/Pnas.0603900103.

vanBreukelen, M., Vonhof, H., Hellstrom, J., Wester, W., Kroon, D., 2008. Fossil dripwater in stalagmites reveals Holocene temperature and rainfall variation in Amazonia. Earth and Planetary Science Letters 275, 54–60. http://dx.doi.org/10.1016/j.epsl.2008.07.060.

Vimeux, F., Gallaire, R., Bony, S., Hoffmann, G., Chiang, J., 2005. What are the climate controls on δD in precipitation in the Zongo Valley (Bolivia)? Implications for the Illimani ice core interpretation. Earth and Planetary Science Letters 240, 205–220. http://dx.doi.org/10.1016/j.epsl.2005.09.031.

Vuille, M., Bradley, R.S., Healy, R., Werner, M., Hardy, D.R., Thompson, L.G., Keimig, F., 2003. Modeling $\delta^{18}O$ in precipitation over the tropical Americas: 2. Simulation of the stable isotope signal in Andean ice cores. Journal of Geophysical Research 108 (D6), 4175. http://dx.doi.org/10.1029/2001JD002039.

Vuille, M., Keimig, F., 2004. Interannual variability of summertime convective cloudiness and precipitation in the central Andes derived from ISCCP-B3 data. Journal of Climate 17, 3334–3348.

Vuille, M., Werner, M., 2005. Stable isotopes in precipitation recording South American summer monsoon and ENSO variability: observations and model results. Climate Dynamics 25, 401–413. http://dx.doi.org/10.1007/S00382-005-0049-9.

Vuille, M., Burns, S.J., Taylor, B.L., Cruz, F.W., Bird, B.W., Abbott, M.B., Kanner, L.C., Cheng, H., Novello, V.F., 2012. A review of the South American monsoon history as recorded in stable isotopic proxies over the past two millennia. Climate of the Past 8, 1309–1321. http://dx.doi.org/10.5194/cp-8-1309-2012.

Wang, Y., Cheng, H., Edwards, R.L., Kong, X., Shao, X., Chen, S., Wu, J., Jiang, X., Wang, X., An, Z., 2008. Millennial- and orbital-scale changes in the East Asian monsoon over the past 224,000 years. Nature 451, 1090–1093. http://dx.doi.org/10.1038/nature06692.